

MeshA*: Efficient Path Planning With Motion Primitives

Marat Agranovskiy¹, Konstantin Yakovlev²

¹St. Petersburg State University

²FRC CSC RAS, AIRI, SPbU

agrinscience@gmail.com, yakovlev.ks@gmail.com

Abstract

We study a path planning problem where the possible move actions are represented as a finite set of motion primitives aligned with the grid representation of the environment. That is, each primitive corresponds to a short kinodynamically-feasible motion of an agent and is represented as a sequence of the swept cells of a grid. Typically heuristic search, i.e. A*, is conducted over the lattice induced by these primitives (lattice-based planning) to find a path. However due to the large branching factor such search may be inefficient in practice. To this end we suggest a novel technique rooted in the idea of searching over the grid cells (as in vanilla A*) simultaneously fitting the possible sequences of the motion primitives into these cells. The resultant algorithm, MeshA*, provably preserves the guarantees on completeness and optimality, on the one hand, and is shown to notably outperform conventional lattice-based planning (x1.5 decrease in the runtime), on the other hand. Moreover, we suggest an additional pruning technique that additionally decreases the search space of MeshA*. The resultant planner is combined with the regular A* to retain completeness and is shown to further increase the search performance at the cost of negligible decrease of the solution quality.

Introduction

Kinodynamic path planning is a fundamental problem in AI, automated planning and robotics. Among the various approaches to tackle this problem the following two are the most widespread and common: sampling-based planning (Karaman and Frazzoli 2011; Sakcak et al. 2019) and lattice-based planning (Pivtoraiko and Kelly 2005; Pivtoraiko, Knepper, and Kelly 2009). The former methods operate in the continuous space, rely on the randomized decomposition of the problem into the smaller sub-problems and are especially advantageous in high-dimensional planning (e.g. planning for robotic manipulators). Still they provide only probabilistic guarantees of the completeness and the optimality. Lattice-based planners rely on the discretization of the workspace/configuration space and provide strong theoretical guarantees w.r.t. this discretization. Consequently, they may be preferable when the number of degrees of freedom of the agent is not high, such as in mobile robotics when one primarily considers the coordinates and the heading of the robot.

This is a pre-print. Currently under review.

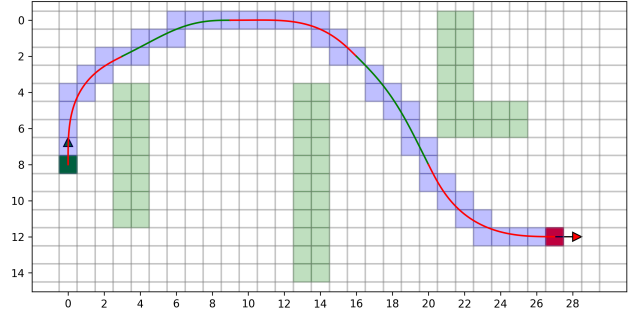


Figure 1: Example of the path planning problem. The workspace is discretized to a grid, where the green cells correspond to the obstacles and the white ones represent the free space. The green cell with an arrow denotes the start state (position and heading), while the red cell – the goal one. The path is composed of the primitives (green and red segments). The swept cells are shown in blue.

Lattice-based planning methods reason over the so-called *motion primitives* – the precomputed kinodynamically-feasible motions from which the sought path is constructed – see Fig. 1. Stacked motion primitives form a *state lattice*, i.e. a graph, where the vertices correspond to the states of the agent and the edges – to the motion primitives. A shortest path on this graph may be obtained by the algorithms, such as A* (Hart, Nilsson, and Raphael 1968), that guarantee completeness and optimality. Unfortunately, when the number of motion primitives is high (which is not uncommon in practice) searching over the lattice graph becomes computationally burdensome. To this end in this work we introduce a novel perspective on the lattice-based planning.

We leverage the assumption that the workspace is represented as an occupancy grid (a standard practice for path planning) and search over this grid in a cell-by-cell fashion to form a sequence of cells such that a sought path, i.e. a sequence of the motion primitives, may be fitted into this sequence of cells. We introduce a dedicated technique to reason simultaneously about the grid cells and the motion primitives that pass through these cells within the search process. Such reasoning allows us to decrease the branching factor, on the one hand, and to maintain the theoretical guarantees,

on the other hand.

Empirically, we show that the introduced path planning method, called MeshA*, is notably (up to 1.5x) faster than the conventional A* and its lazy variant (this holds when the weighted heuristic is utilized as well). We also introduce an additional pruning technique that decreases the search space of MeshA*. The planner employing this technique is not complete but can be combined with the regular A* to retain completeness. The resultant hybrid planner is shown to further increase the search performance (compared to MeshA*) with a negligible decrease in solution quality.

Related Work

A variety approaches to path finding with taking kinodynamic constraints of the mobile agent into account exists (González et al. 2016). One of the prominent approaches is sampling-based planning. The classical representative is RRT algorithm (LaValle and Kuffner 2001) that rapidly explores the configuration space. Its anytime modification, RRT* (Karaman and Frazzoli 2010), gradually improve the solution and is aimed at converging to optimal solutions. Informed RRT* (Gammell, Srinivasa, and Barfoot 2014) applies heuristics to enhance efficiency. RRT-Connect (Kuffner and LaValle 2000) is a fast bidirectional planner. RRT^X is an adaptation of RRT tailored to fast re-planning needed for navigation of an agent in unpredictably changing environment.

Another approach is the lattice-based planning when a set of motion primitives, that respect the constraints of the agent, is constructed and then a search for a suitable sequence of such primitives is conducted. To compose primitives various approaches are proposed, such as B-splines (Flores and Milam 2006), the shooting method (Jeon, Karaman, and Frazzoli 2011), the covering method (Yakovlev et al. 2022), learning techniques (De Iaco, Smith, and Czarnecki 2019), and others. In this work, we follow the lattice-based approach but do not focus on constructing the primitives themselves and consider them to be given (in the experiments we use a simple Newton’s optimization method (Nagy and Kelly 2001) to obtain primitives for a car-like agent).

In this work we focus on reducing the search efforts in path planning. Numerous algorithms aimed at the similar goals have already been developed, such as Jump Point Search (Harabor and Grastien 2011), which significantly accelerates search on an 8-connected grid, and the well-known WA* (Ebendt and Drechsler 2009), which provides suboptimal solutions through the use of weighted heuristics.

Problem Statement

Consider a point-sized mobile agent that moves in a 2D workspace $W \subset \mathbb{R}^2$ that is composed of the free space, W_{free} , and the obstacles, W_{obs} , and is tessellated into the grid (composed of the square cells). A grid cell, denoted as (i, j) , is considered blocked if its intersection with W_{obs} is not empty, and is free otherwise.

State Representation. The state of the agent is defined by a 3D vector (x, y, ϕ) , where $(x, y) \in W$ are the coordi-

inates in the workspace and $\phi \in [0, 360^\circ)$ is the heading angle. We assume that the latter can be discretized into a set $\Theta := \{\phi_1, \dots, \phi_k\}$, allowing us to focus on discrete states $s := (i, j, \theta)$ that correspond to the centers of the grid cells $(i, j) \in \mathbb{Z}^2$, with $\theta \in \Theta$.

Motion Primitives. The kinematic constraints and physical capabilities of the mobile agent are encapsulated in *motion primitives*, each representing a short kinodynamically-feasible motion (i.e., a continuous state change). We assume that these primitives align with the discretization, meaning that transitions occur between two discrete states, such as (i, j, θ) and (i', j', θ') . In other words, the motion starts at the center of a grid cell, ends at the center of another cell, and the agent’s heading at the endpoints belongs to a finite set of possible headings. Each primitive is additionally associated with the *collision trace*, which is a sequence of cells swept by the agent when execution the motion, and *cost* which is a positive number (e.g. the length of the primitive).

For a given state $s = (i, j, \theta)$ there is a finite number of motion primitives that the agent can use to move to other states. Moreover, we assume that there can be no more than one primitive leading to each other state, which corresponds to the intuitive understanding of a primitive as an elementary motion. We also consider that the space of discrete states, along with the primitives, is *regular*; that is, for any $\delta_i, \delta_j \in \mathbb{Z}$ if there exist a motion primitive connecting (i, j, θ) and (i', j', θ') then there also exists one from $(i + \delta_i, j + \delta_j, \theta)$ to $(i' + \delta_i, j' + \delta_j, \theta')$. While the endpoints of such primitives are distinct, the motion itself is not. This means that the collision traces of these primitives differ only by a parallel shift of the cells, and their costs coincide.

Thus, we can consider a canonical set of primitives – *control set* – from which all others can be obtained through parallel translation. We assume that such set is finite and is computed in advance according to the specific motion model of the mobile agent. To avoid any misunderstanding, we clarify that the term “primitive” and the corresponding notation *prim* will be used in two contexts:

- When we refer to a primitive, we mean a specific motion between discrete states.
- When we specify that a primitive is *from the control set*, we mean a motion template that, when instantiated from a specific discrete state, yields an exact primitive.

Path. A *path* is a sequence of motion primitives, where the adjacent ones share the same discrete state. The path’s *collision trace* is the union of the collision traces of the constituent primitives (shown as blue cells in Fig. 1). A path is considered *collision-free* if its collision trace consists of the free cells only.

Problem. Our task is to construct a collision-free path between the two given discrete states: the start one, s_0 , and the goal one, s_f . We wish to solve this problem optimally, i.e. to obtain the least cost path, where the cost of the path is the sum of costs of the primitives forming the path.

Method

A well-established approach to solve the given problem is to search for a path on a *state lattice* graph, where the ver-

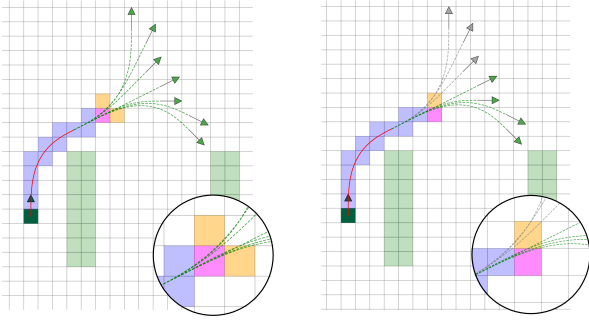


Figure 2: Definition of cell successors during the construction of a collision trace.

tices represent the discrete states and edges – the primitives connecting them. In particular, heuristic search algorithms of the A* family can be used for such pathfinding.

These algorithms iteratively construct a search tree composed of the partial paths (sequences of the motion primitives). At each iteration the most prominent partial path is chosen for extension. Extension is done by expanding the path’s endpoint – a discrete state (i, j, θ) . This expansion involves considering all the primitives that can be applied to the state, checking which ones are valid (i.e. do not collide with the obstacles), computing the transition costs, filtering out the duplicates (i.e. the motions that lead to the states for which there already exist paths in the search tree at a lower cost) and adding the new states to the tree. Indeed, as the number of available motion primitives increases the expansion procedure (which is the main building block of a search algorithm) becomes computationally burdensome and the performance of the algorithm degrades.

Partially, this problem can be addressed by the *lazy* approach, where certain computations associated with the expansion are postponed, most often – collision checking. However, in environments with complex obstacle arrangements, searches that exploit lazy collision checking often extract invalid states (for which the collision check fails). Consequently, a significant amount of time is wasted on extra operations with the search tree, which is also time-consuming.

We propose an alternative approach. We abandon the search at the level of primitives and instead conduct the search at the level of cells, where the number of successors is limited and does not depend on the amount of motion primitives. During the search, we simultaneously reason about the possible motion primitives that can pass through the cells. This is achieved through careful organization of the search space (i.e. we introduce a search element that is a combination of a cell and a set of primitives) and a proper definition of the successor relationship. As a result we are able to obtain optimal solutions faster leveraging the cell-by-cell nature of the search process.

To gain an intuition about how our search operates, consider an example illustrated in Fig. 2. On the left, we see a partial collision trace that ends with a magenta cell – a cell that is under expansion. Assume that we know this cell can be reached by first applying the red primitive in the start

state, followed by any of the green primitives (as their collision traces do not differ before reaching this cell). We store information about the primitives that pass through a cell, and this augmentation is called an *extended cell* (which is central to our approach and will be formally defined later). With this information, we can infer that the cell under expansion may have two successors (the ones that follow it along the green primitives) – the cells depicted in orange. We generate the corresponding extended cells as successors, propagating the information about the primitives that pass through them. At a later stage of the search, one of these cells is chosen for expansion – the one to the right (see the right part of Fig. 2). As the information on the motion primitives was propagated from its predecessor (note that the gray ones are not included in this information, as they led to a different cell from the predecessor), we can again establish which of the adjacent grid cells may serve as the continuation of the collision trace – the cell above the expanding one.

This example highlights the main idea of our approach – conducting the search at the level of cells while simultaneously reasoning over the motion primitives that pass through them. Next, we describe it in more details.

The Search Space

The element of our search space is an **extended cell**. Formally it is a tuple:

$$u = (i, j, \Psi), \text{ where}$$

- (i, j) is a grid cell,
- $\Psi = \{(prim_1, k), (prim_2, k), \dots, (prim_n, k) \mid \forall l \in [1, n] : 1 \leq k < U_{prim_l}\}$ is a

set of pairs consisting of a primitive from the control set and the non-maximum index in its collision trace.

Here U_{prim} is the number of cells in the collision trace of the primitive $prim$.

To better understand the definition, recall that the primitives from the control set are considered as the motion templates, which, when copied into a specific discrete state, yield a particular primitive. Thus, the conceptual meaning of this definition is as follows: for each pair $(prim, k) \in \Psi$, we consider a copy of $prim$ that traverses the cell (i, j) , in such a way that it is the k -th cell in the collision trace of that primitive. Consequently, the extended cell captures the information about the grid cell itself and the motion primitives that pass through it. Importantly, the index k is the same across all the primitives “stored” in an extended cell. In Fig. 2, the magenta cells with the green primitives passing through them are the examples of the extended cells.

The *projection* of the extended cell $u = (i, j, \Psi)$ will be referred to as the cell with the coordinates (i, j) . The set Ψ will be referred to as the *configuration of primitives*. In practice, instead of storing such a complex structure directly in an extended cell a single number can be used, obtained by numbering the configurations of primitives (more details on this are in the Appendix).

Initial extended cells

As will be shown later, it is important for us to distinguish a special class of the configurations of primitives called *initial*.

Algorithm 1: Building the Initial Configuration

Input: Discrete angle θ **Output:** Initial configuration for this angle**Function name:** `InitConf(θ)`

```
1:  $\Psi \leftarrow \emptyset$ 
2: for all  $prim \in$  control set do
3:   if  $prim$  emerges in  $\theta$  then
4:      $\Psi.add((prim, 1))$ 
5:   end if
6: end for
7: return  $\Psi$ 
```

To introduce this term, consider a specific heading $\theta \in \Theta$. Now the initial configuration of the primitives for this heading is defined as:

$$\Psi_\theta := \{(prim_1, 1), \dots, (prim_r, 1)\},$$

where $prim_1, \dots, prim_r$ are all the primitives from the control set that start with heading θ . To get the initial configuration a straightforward algorithm – see Alg. 1 – is used.

If some extended cell is defined via (contains) the initial configuration of primitives such cell is also called an *initial extended cell*.

Successors

To define the successor relationship between the extended cells let us first denote by

$$\Delta_k^{prim} := (i' - i, j' - j)$$

the change in the grid coordinates that occurs when transitioning from the k -th cell to the $(k+1)$ -th cell in the collision trace of some primitive $prim$. This change will be referred to as the *step along the primitive*.

Let $u = (i, j, \Psi)$ and $v = (i', j', \Psi')$ be two extended cells. How can v be a successor of u ? Intuitively, the successors of an extended cell are obtained simply as the results of steps along each primitive from the configuration (as illustrated in Fig. 2). To formally define the successor relationship, it is necessary to consider the following two cases:

1. Let v be the initial extended cell, all primitives in which emerge at an angle θ (i.e., $\Psi' = \Psi_\theta$). Then v is a *successor* of u (we will also use term *initial successor* for v) if the following condition holds:

$$\exists(prim, k) \in \Psi \text{ such that: } k = U_{prim} - 1,$$

$$\Delta_k^{prim} = (i' - i, j' - j) \text{ and } prim \text{ ends at angle } \theta$$

This condition requires that there exists a primitive $prim$ in Ψ for which the cells (i, j) and (i', j') are the last ones in the collision trace. In this case, at the cell (i', j') , we can consider its extension by a whole bundle of primitives that begin at the same angle θ at which $prim$ ends.

2. If v is not the initial extended cell, then v is a *successor* of u if the following conditions are simultaneously satisfied:

- (a) $\forall(prim, k) \in \Psi'$ the following holds:

$$(prim, k - 1) \in \Psi \text{ and } (i' - i, j' - j) = \Delta_{k-1}^{prim}$$

Algorithm 2: Generating Successors of an Extended Cell

Input: Extended cell u **Output:** Set of pairs of successors and transition costs**Function name:** `GetSuccessors(u)`

```
1:  $i, j, \Psi \leftarrow u$ 
2:  $Conf s \leftarrow \{\}$  ▷ Dictionary
3:  $Successors \leftarrow \emptyset$  ▷ Set of successors and costs
4: for all  $(prim, k) \in \Psi$  do
5:    $(a, b) \leftarrow \Delta_k^{prim}$ 
6:   if  $k = U_{prim} - 1$  then ▷ Case 1
7:      $\theta \leftarrow$  angle at which  $prim$  ends
8:      $\Psi_1 \leftarrow$  InitConf( $\theta$ )
9:      $v_1 \leftarrow (i + a, j + b, \Psi_1)$ 
10:     $Successors.add((v_1, c_{prim}))$ 
11:   else if  $(a, b) \notin Conf s$  then ▷ Case 2
12:      $conf_{new} \leftarrow \{(prim, k + 1)\}$ 
13:      $Conf s[(a, b)] \leftarrow conf_{new}$ 
14:   else
15:      $Conf s[(a, b)].add((prim, k + 1))$ 
16:   end if
17: end for
18: for all  $(a, b) \in Conf s$  do
19:    $\Psi_2 \leftarrow Conf s[(a, b)]$ 
20:    $v_2 \leftarrow (i + a, j + b, \Psi_2)$ 
21:    $Successors.add((v_2, 0))$ 
22: end for
23: return  $Successors$ 
```

- (b) $\forall(prim, k) \in \Psi$ such that $k < U_{prim} - 1$ and $\Delta_k^{prim} = (i' - i, j' - j)$ the following holds:
 $(prim, k + 1) \in \Psi'$

Condition (b) requires that all primitives of the predecessor leading to the projection cell of the successor are present in its configuration, while Condition (a) ensures that there are no other primitives in the successor.

Having defined the successor relationship, we now define the cost of transitioning from a predecessor to a successor, assuming that the cost of each primitive $prim$ is c_{prim} .

Let $u = (i, j, \Psi)$ and $v = (i', j', \Psi')$ be two extended cells, where v is a successor of u . The cost of the transition from u to v is:

- $cost(u, v) = 0$ if v is not an initial cell
- $cost(u, v) = c_{prim}$ where $prim$ is such that $(prim, U_{prim} - 1) \in \Psi$, $\Delta_{U_{prim} - 1}^{prim} = (i' - i, j' - j)$ and $prim$ ends at angle θ (where $\theta : \Psi' = \Psi_\theta$), otherwise

Note that in the second case, such a primitive exists by the definition of the initial successor. If there are multiple such primitives, the cost associated with any of them can be chosen as $cost(u, v)$. In fact, it will be shown in the next section that such ambiguity cannot exist.

The pseudocode of the procedure that generates successors for an extended cell and sets the costs appropriately is given in Algorithm 2.

MeshA*

Having defined the elements of the search space as well as the successor relationship, we obtain a directed weighted graph that we will call the *mesh graph*. We can utilize a standard heuristic search algorithm, i.e. A*, to search for a path on this graph. We will refer to this approach as *MeshA**. Next we will show that running MeshA* leads to finding the optimal solution of the problem at hand, which is equivalent to the one found by A* on the lattice graph.

Theoretical Results

In this section, we will demonstrate the equivalence between searches on the mesh graph we constructed and those on the state lattice. The main result is Theorem 3, which outlines the recipe for trajectory construction.

Note: to distinguish between a path as a sequence of vertices (where adjacent vertices are connected by an edge) in a certain graph and a path as a sequence of motion primitives, we will refer to the latter as the *trajectory*.

Lemma 1. *Let an extended cell $u = (i, j, \Psi)$ be given, and let the cell (i', j') be such that it is the result of a step along one of the primitives from u , that is:*

$$\exists (prim, k) \in \Psi : \Delta_k^{prim} = (i' - i, j' - j)$$

Then there exists a configuration of primitives Ψ' such that the extended cell $v := (i', j', \Psi')$ will be a successor of u . Moreover, Ψ' can always be composed in such a way that it is non-initial, except in the case when $k = U_{prim} - 1$.

In the latter case, $\Psi' := \Psi_\theta$ (where $prim$ ends at the angle θ) will satisfy the lemma.

Lemma 2. *For any path u_1, u_2, \dots, u_N on the mesh graph starting from an initial extended cell, the following holds:*

1. *For any another initial extended cell u_l with $l > 1$ on this path, if all primitives of its configuration exit at some angle θ (i.e., $\Psi_l = \Psi_\theta$), then there exists a unique $(prim, k) \in \Psi_{l-1}$ such that $prim$ ends at angle θ , $k = U_{prim} - 1$, and $\Delta_k^{prim} = (i_l - i_{l-1}, j_l - j_{l-1})$.*
2. *The costs of all transitions along the path are uniquely defined.*

Note that here we use the notation $u_l := (i_l, j_l, \Psi_l)$.

The meaning of point 1 is that among the primitives in Ψ_{l-1} , there is only one that ensures u_l is a successor of u_{l-1} (i.e., removing this primitive from configuration Ψ_{l-1} would cause u_l to no longer be a successor of u_{l-1}).

The proofs of Lemmas 1 and 2 are straightforward and omitted for the sake of space. They can be found in the Appendix.

Theorem 1. *Let there be an edge in the state lattice graph, that is, some primitive $prim$ that transitions from one discrete state $s_a = (i_a, j_a, \theta_a)$ to another $s_b = (i_b, j_b, \theta_b)$. In this case, there exists a path in the mesh graph from the initial extended cell $(i_a, j_a, \Psi_{\theta_a})$ to another initial cell $(i_b, j_b, \Psi_{\theta_b})$ that satisfies the following conditions:*

1. *The projections of the vertices along this path precisely form the collision trace of this primitive.*
2. *The cost of this path is exactly equal to the cost of the primitive c_{prim} .*

Proof. First, we note that, similar to the state lattice, the mesh graph is regular. That is, if there is a path between the extended cells (i_1, j_1, Ψ_1) and (i_2, j_2, Ψ_2) , then there is also a path between all pairs $(i_1 + \delta_i, j_1 + \delta_j, \Psi_1)$ and $(i_2 + \delta_i, j_2 + \delta_j, \Psi_2)$ for any integers δ_i and δ_j . This straightforwardly follows from the definition of the successor relation on the mesh graph, which is independent of the coordinates due to the regularity of the state lattice. Therefore, it suffices to prove the statement assuming that $prim$ is a primitive from the control set.

For convenience, we will use the notation $n = U_{prim}$. Let the collision trace of the $prim$ consists of cells $(i_1, j_1), (i_2, j_2), \dots, (i_n, j_n)$ (with indexing following the order of traversal along the primitive). From the condition, it follows that $i_1 = i_a, j_1 = j_a$ and $i_n = i_b, j_n = j_b$.

Now, let us consider the extended cell $u_1 = (i_1, j_1, \Psi_{\theta_a})$. Since the primitive exits at an angle θ_a , it follows from the definition of the initial configuration of primitives that $(prim, 1) \in \Psi_{\theta_a}$. Next, we observe that each cell (i_k, j_k) results from a step along the primitive $prim$ from the cell (i_{k-1}, j_{k-1}) , as they sequentially follow in the collision trace of this primitive. Thus, by Lemma 1, for the extended cell u_1 and the cell (i_2, j_2) , there exists a non-initial extended cell $u_2 = (i_2, j_2, \Psi_2)$ that is a successor of u_1 . By the definition of a non-initial successor, we get $(prim, 2) \in \Psi_2$.

We can continue to apply Lemma 1 analogously, leading to the conclusion that for all $n - 1 \geq k \geq 2$, there exists a non-initial extended cell u_k that is a successor of u_{k-1} and $(prim, k) \in \Psi_k$. It remains to note that for the extended cell u_{n-1} and the cell (i_n, j_n) , Lemma 1 also provides a successor, which is the initial cell $u_n = (i_n, j_n, \Psi_{\theta_b})$, where the angle θ_b is precisely the angle at which $prim$ ends.

Finally, we obtain a sequence u_1, u_2, \dots, u_n where each extended cell is a successor of the previous one, thus forming a path in the mesh graph. Since the projection u_k is exactly (i_k, j_k) (the k -th cell of the collision trace of the primitive), the first point of the theorem is proven.

To prove the second part, we note that in the considered path on the mesh graph, all transitions except the last lead to non-initial extended cells, meaning the costs of these transitions are equal to 0. The last transition occurs from the extended cell $u_{n-1} = (i_{n-1}, j_{n-1}, \Psi_{n-1})$ to the initial extended cell $u_n = (i_n, j_n, \Psi_{\theta_b})$. Since u_{n-1} and u_n are on the path from the initial extended cell u_1 , according to Lemma 2, the cost of transitioning from u_{n-1} to u_n is uniquely defined. Since $(prim, n - 1) \in \Psi_{n-1}$, $\Delta_{n-1}^{prim} = (i_n - i_{n-1}, j_n - j_{n-1})$, and $prim$ ends at the angle θ_b , in our case, this transition cost is exactly c_{prim} . This completes the proof of the second part. \square

Theorem 2. *Let two initial extended cells $u = (i, j, \Psi_\theta)$ and $u' = (i', j', \Psi_{\theta'})$ be fixed. Suppose there exists a path in the mesh graph from the first one to the second one. Then, there will be a trajectory composed of primitives (corresponding to the path in the state lattice) that transitions from the discrete state $s = (i, j, \theta)$ to $s' = (i', j', \theta')$ and satisfies the following conditions:*

1. *The collision trace of this trajectory coincides with the projections of the vertices along this mesh graph path.*

2. The cost of this trajectory is equal to the cost of the path in the mesh graph.

Proof. We will prove the statement by mathematical induction on the number of initial extended cells along the specified path in the mesh graph. For one initial extended cell, the case is trivial, resulting in an empty trajectory.

Let u_1, u_2, \dots, u_N be the path in the mesh graph as specified, where u_k denotes the extended cell (i_k, j_k, Ψ_k) , with $u_1 = u$ and $u_N = u'$ being the initial extended cells from the condition. According to Lemma 2, all transition costs along this path are uniquely defined (which means that point 2 of the theorem is at least correctly formulated). Additionally, since u_N is initial and a successor of u_{N-1} , there exists a unique (according to Lemma 2) primitive $prim$ from the control set such that $(prim, U_{prim} - 1) \in \Psi_{N-1}$, $prim$ ends at angle θ' and (i_N, j_N) is the result of a step along $prim$ from (i_{N-1}, j_{N-1}) . In this case, the cost of transitioning from u_{N-1} to u_N is equal to c_{prim} .

Next, using the definition of a non-initial successor, we find that since u_{N-1} is a successor of u_{N-2} , it follows that $(prim, U_{prim} - 2) \in \Psi_{N-2}$ and the step along $prim$ from (i_{N-2}, j_{N-2}) leads to (i_{N-1}, j_{N-1}) . Continuing this process, we obtain that for all $U_{prim} - 1 \geq k \geq 1$, it holds that $(prim, k) \in \Psi_{N-U_{prim}+k}$ and $(i_{N-U_{prim}+k+1}, j_{N-U_{prim}+k+1}, \Psi_{N-U_{prim}+k+1}) = \Delta_k^{prim}$.

This result leads to two conclusions. First, if a copy of $prim$ (considered as a motion template) is placed at $(i_{N-U_{prim}+1}, j_{N-U_{prim}+1})$, then for the resulting primitive, the sequence of cells $(i_{N-U_{prim}+1}, j_{N-U_{prim}+1}), \dots, (i_N, j_N)$ forms its collision trace, as each cell in this sequence is the result of a step along the primitive from the previous cell. Second, since $(prim, 1) \in \Psi_{N-U_{prim}+1}$, it follows that the extended cell $u_{N-U_{prim}+1}$ is initial, because according to the definition of successors, this is the only case in which the configuration of primitives (of some extended cell that is a successor of another one) can include a primitive paired with the index 1 in its collision trace. Thus, we obtain that $\Psi_{N-U_{prim}+1} = \Psi_\phi$, where the primitive $prim$ exits at an angle ϕ .

As a result, we have a sequence of extended cells $u_1, u_2, \dots, u_{N-U_{prim}+1}$ that also forms a path in the mesh graph between the initial extended cells $u_1 = u = (i, j, \Psi_\theta)$ and $u_{N-U_{prim}+1} = (i_{N-U_{prim}+1}, j_{N-U_{prim}+1}, \Psi_\phi)$, but contains one fewer initial extended cell than the original path. This allows us to apply the induction hypothesis and conclude that there exists a trajectory composed of primitives that transitions from the discrete state $s = (i, j, \theta)$ to $t = (i_{N-U_{prim}+1}, j_{N-U_{prim}+1}, \phi)$, satisfying all the requirements of the theorem.

Since this trajectory ends at the angle ϕ , at which $prim$ begins, and since, as previously discussed, we can consider the primitive obtained by copying $prim$ at $(i_{N-U_{prim}+1}, j_{N-U_{prim}+1})$, then we can append it to the end of this trajectory to obtain a trajectory that transitions from the discrete state s to s' (with a cost that increases by exactly c_{prim}). It corresponds to the original path in the

Algorithm 3: Trajectory Reconstruction

Input: Path u_1, u_2, \dots, u_N in the mesh graph between initial extended cells.

Output: Trajectory (chain of primitives).

```

1:  $Traj \leftarrow \emptyset$ 
2:  $p = u_1$ 
3: for all  $l = 2, 3, \dots, N$  do
4:   if  $u_l$  is initial then  $\triangleright u_l$  are next initial after  $p$ 
5:      $i_1, j_1, \Psi_{\theta_1} \leftarrow p$ 
6:      $i_2, j_2, \Psi_{\theta_2} \leftarrow u_l$ 
7:      $s_1 \leftarrow (i_1, j_1, \theta_1)$   $\triangleright$  Obtain discrete states.
8:      $s_2 \leftarrow (i_2, j_2, \theta_2)$ 
9:      $prim \leftarrow$  primitive from  $s_1$  to  $s_2$ 
10:     $Traj.add(prim)$ 
11:     $p = u_l$ 
12:   end if
13: end for
14: return  $Traj$ 

```

mesh graph and obviously satisfies all the requirements of the theorem. This concludes the proof. \square

Theorem 3 (Main Theorem). *The search for a path in the state lattice graph is equivalent to the search for a path in the mesh graph in the following sense: to find a trajectory between the discrete states $s = (i, j, \theta)$ and $s' = (i', j', \theta')$ with a cost c , it is sufficient to perform two steps:*

1. Find a path with cost c in the mesh graph between the initial extended cells $u = (i, j, \Psi_\theta)$ and $u' = (i', j', \Psi_{\theta'})$.
2. Recover the trajectory from s to s' based on the found path using Algorithm 3.

The proof of Theorem 3 involves a meticulous combination of previous results and is therefore omitted here. It can be found in the Appendix.

Soft Duplicates Pruning

As postulated above the main ingredient of MeshA* is the extended cell, which is a tuple (i, j, Ψ) . For two extended cells, (i, j, Ψ) and (i', j', Ψ') , to be equal all their elements should coincide. That is $i = i', j = j', \Psi = \Psi'$. This definition is used in MeshA* for detecting duplicates.

Consider now two extended cells for which $i = i', j = j', \Psi \neq \Psi'$, but most of the elements forming Ψ and Ψ' coincide. In other words, the extended cells share the coordinates but slightly differ in their constituting primitives. Intuitively, these extended cells are quite similar and can be considered *soft duplicates* and one can prune such duplicates in the search tree. We will dub an algorithm that utilizes such pruning of the soft duplicates as *Mesh/PruningA**.

The specific rule for determining soft duplicates is left to the user, as it should be tailored based on preferences and experimental results. For our evaluations, we chose the following approach. For each extended cell in the mesh graph, we considered the set of vertices reachable from it in ≤ 2 steps (i.e., those for which there is a path consisting of no

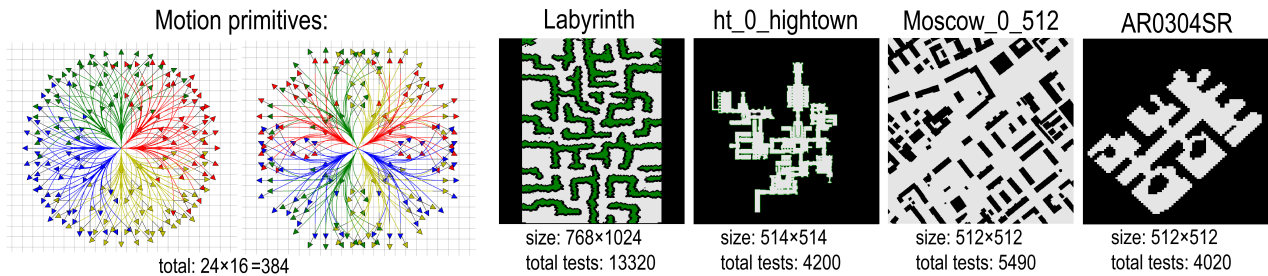


Figure 3: Experimental setup: control set and MovingAI maps.

more than 2 edges), and then projected these vertices to obtain a corresponding set of grid cells. We considered vertices with shared coordinates as soft duplicates if their associated sets of grid cells coincide. In practice, it is sufficient to compare two numbers obtained from the enumeration of these sets (details can be found in the Appendix).

Indeed, *Mesh/PruningA** might consider less search nodes in practice due to pruning (and thus find a solution faster) but, evidently, it is incomplete in general. To this end we suggest to combine *Mesh/PruningA** and regular *A** that operates in the space of original motion primitives (not the extended cells) and is complete and optimal. That is we interleave two searches: after K steps of *Mesh/PruningA**, where K is a user-defined parameter, we perform one step of regular *A**. In our experiments we set K to 100. We refer to such an approach as *Mesh/ParallaA**. Obviously, it is complete (as we have now regular *A** in the loop). Still, the optimality of the solution is not guaranteed. However, we expect that in practice the cost overhead will be low. This expectation is confirmed by our empirical evaluation.

Empirical Evaluation

Setup. In the experiments we utilize 16 different headings and generate 24 motion primitives for each heading. We generate the primitives using the motion model of a car-like robot. We use four maps of varying topology from the well-known MovingAI benchmark (Sturtevant 2012) for the experiments. The start and goal locations on these maps were picked from the scenario files that are present in the benchmark. For any pair of start-goal locations we randomly generate three different headings. The total number of instances across all the maps exceeds 25000. Fig. 3 provides an overview of our setup.

The following algorithms were evaluated:

1. **LBA*** (short for Lattice-based A*): The standard A* algorithm on the state lattice, serving as the baseline.
2. **LazyLBA***: The same algorithm that conducts collision-checking lazily.
3. **MeshA*** (ours): Running A* on the mesh graph.
4. **Mesh/ParallaA*** (ours): An algorithm that combines Mesh/PruningA* and LBA*.

The cost of each primitive is defined as its length, and the heuristic function is the Euclidean distance. We use five different weights for this heuristic in our experiments: $w =$

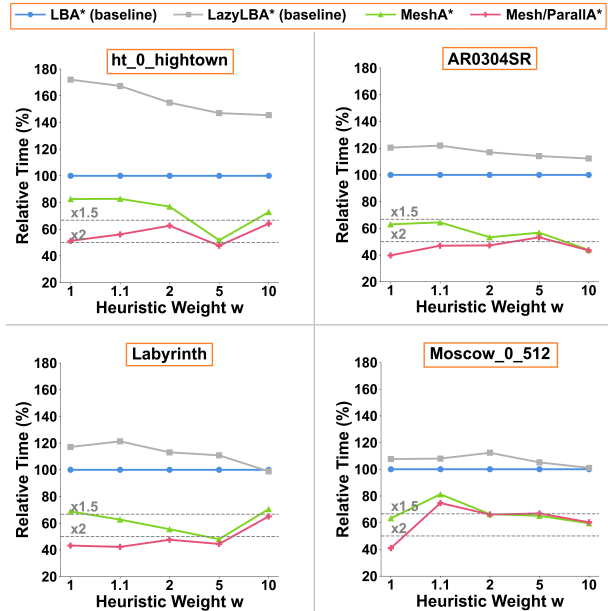


Figure 4: Median runtime of the evaluated algorithms (relative to the runtime of LBA*). The lower – the better. 50% corresponds to x2 speed-up.

1, 1.1, 2, 5, 10. It is known that utilizing weighted heuristic speeds up the search (Ebdndt and Drechsler 2009) while the cost of the solution increases.

Results. Fig. 4 illustrates the median runtime of each algorithm as a ratio to the runtime of LBA*. That is the runtime of LBA* is considered 100% in each run and the runtime of the other solvers is divided by this value. Thus the lower the line is on the plot – the better. Clearly MeshA* consistently outperforms the baselines. For $w = 1$ it consumes on average 60%-80% of the LBA* runtime (depending on the map). That is the speed-up is up to 1.5x. When the heuristic is weighted this gap can get even more pronounced and we can observe x2 speed-up. Next, Mesh/ParallaA* is notably faster than MeshA* for lower heuristic weights. For higher weights the runtime of MeshA* and Mesh/ParallaA* is similar. This phenomenon occurs because, at higher values of w , the speed of solving the tests increases to the point where the benefits of additional pruning in Mesh/ParallaA* become less noticeable, overshadowed by the overhead of alternat-

Algorithms	Labyrinth				ht_0_hightown				Moscow_0_512			
	$w = 1$	$w = 2$	$w = 5$	$w = 10$	$w = 1$	$w = 2$	$w = 5$	$w = 10$	$w = 1$	$w = 2$	$w = 5$	$w = 10$
LBA*	100.0	105.4	109.9	112.3	100.0	105.7	110.0	113.2	100.0	105.9	108.9	110.8
LazyLBA*	100.0	105.4	109.9	112.3	100.0	105.7	110.0	113.2	100.0	105.9	108.9	110.8
MeshA*	100.0	110.8	122.6	128.6	100.0	109.2	117.6	122.3	100.0	113.3	125.2	131.4
Mesh/ParallA*	100.5	111.1	123.0	128.8	100.7	109.7	117.7	122.7	100.3	113.6	124.9	130.9

Table 1: The median costs of the obtained solutions in percent (100% = optimal cost).

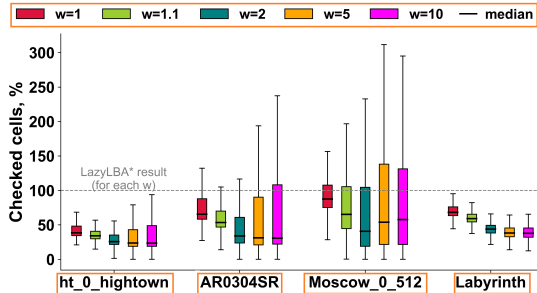


Figure 5: The number of collision checks (1 collision check = estimating the traversability of a single grid cell) for MeshA* relative to the same number of LazyLBA*

ing between the two searches. This effect is particularly pronounced on the `Moscow_0_512`, which features ample open space and no dead ends.

Interestingly, LazyLBA* consistently performs worse than LBA*. This can be attributed to the simplicity of collision checking in our experiments, which involves verifying that the cells in the collision trace of each primitive are not blocked. This is a quick check in our setup and postponing it does not make sense. Moreover, lazy collision checking begin to incur additional time costs from numerous pushing and popping unnecessary vertices to the search queue, which standard LBA* prunes through collision checking. This effect is especially visible on the `ht_0_hightown` map, which contains numerous narrow corridors and passages where many primitives lead to collisions.

The costs of the obtained solutions are summarized in Table 1. Here each cell shows the median cost of the solutions found by a respective algorithms relative to the optimal cost. Thus all the numbers are higher or equal 100%. The lower – the better (100% corresponds to the best possible solutions). Indeed LBA*, LazyLBA* and MeshA* always provide optimal solutions. Evidently, Mesh/ParallA* slightly lags behind MeshA*. Recall however that it is notably faster (for lower heuristic weights). A fractions of percent of cost overhead is a reasonable price for this speed-up.

Another observation is that the cost of the suboptimal solutions found by MeshA* increases more with rising w compared to LBA*. Possibly, this is due to the fact that in the state lattice search, the heuristic function is computed only twice for each primitive (at its start and end), whereas in the mesh graph search, the heuristic is calculated much more frequently – essentially at every cell in the collision trace

of the primitives. Consequently, the increase in the heuristic due to the rise in w has a more pronounced effect on the mesh graph search, resulting in higher costs for the found trajectories.

Finally, we have also analyzed the number of collision checks performed by MeshA* and compare it with the one of LazyLBA*. In our setup, this check involves determining the presence of an obstacle in a grid cell; however, in different practical application, it can be much more labor-intensive (e.g., if sensor queries are required), making a lower number of such checks a significant advantage. Figure 5 presents the results. Clearly, MeshA* demonstrates a significant advantage over LazyLBA*. This is because LazyLBA* frequently extracts invalid vertices (i.e., those obtained from primitives that have collisions), leading to a substantial number of primitive examinations (with collision verification) in the search for a valid one. In contrast, MeshA* operates cell-by-cell, preemptively eliminating all successors at each occupied cell. The advantage of MeshA* is less pronounced on `Moscow_0_512`, which can be attributed to the simplicity of the obstacle arrangement: ample open space and convex obstacles (thus LazyLBA* does not often extract invalid states).

Overall, our experiments confirm that the suggested search approach, MeshA*, consistently outperforms the baselines and is much faster in practice (1.5x faster when searching for optimal solutions and 2x faster when searching for the suboptimal ones). Moreover, if one tolerates a negligible increase in solution cost, Mesh/ParallA*, can speed-up the search even further.

Conclusion

In this paper we have considered a problem of finding a path composed of the motion primitives that are aligned with the grid representation of the workspace. We have suggested a novel way to systematically search for a solution by reasoning over the sequences of augmented grid cells rather than sequences of motion primitives. The resultant solver, MeshA*, is provably complete and optimal and is notably faster than the regular A* that searches in the space of motion primitives.

Despite we have considered path planning in 2D when the agent’s state is defined as (x, y, θ) , the idea that stands behind MeshA* is applicable to pathfinding in 3D as well as to the cases where the agent’s state contains additional variables as long as they can be discretized. Adapting MeshA* to such setups is a prominent direction for future work.

References

- De Iaco, R.; Smith, S. L.; and Czarnecki, K. 2019. Learning a Lattice Planner Control Set for Autonomous Vehicles. In *2019 IEEE Intelligent Vehicles Symposium (IV)*, 549–556.
- Ebendt, R.; and Drechsler, R. 2009. Weighted A* search – unifying view and application. *Artificial Intelligence*, 173(14): 1310–1342.
- Flores, M.; and Milam, M. 2006. Trajectory generation for differentially flat systems via NURBS basis functions with obstacle avoidance. In *2006 American Control Conference*, 7 pp.–.
- Gammell, J. D.; Srinivasa, S. S.; and Barfoot, T. D. 2014. Informed RRT*: Optimal sampling-based path planning focused via direct sampling of an admissible ellipsoidal heuristic. In *2014 IEEE/RSJ International Conference on Intelligent Robots and Systems*, 2997–3004.
- González, D.; Pérez, J.; Milanés, V.; and Nashashibi, F. 2016. A Review of Motion Planning Techniques for Automated Vehicles. *IEEE Transactions on Intelligent Transportation Systems*, 17(4): 1135–1145.
- Harabor, D. D.; and Grastien, A. 2011. Online Graph Pruning for Pathfinding On Grid Maps. *Proceedings of the AAAI Conference on Artificial Intelligence*.
- Hart, P. E.; Nilsson, N. J.; and Raphael, B. 1968. A Formal Basis for the Heuristic Determination of Minimum Cost Paths. *IEEE Transactions on Systems Science and Cybernetics*, 4(2): 100–107.
- Jeon, J. h.; Karaman, S.; and Frazzoli, E. 2011. Anytime computation of time-optimal off-road vehicle maneuvers using the RRT*. In *2011 50th IEEE Conference on Decision and Control and European Control Conference*, 3276–3282.
- Karaman, S.; and Frazzoli, E. 2010. Incremental Sampling-based Algorithms for Optimal Motion Planning. *ArXiv*, abs/1005.0416.
- Karaman, S.; and Frazzoli, E. 2011. Sampling-based algorithms for optimal motion planning. *The International Journal of Robotics Research*, 30(7): 846–894.
- Kuffner, J. J.; and LaValle, S. M. 2000. RRT-connect: An efficient approach to single-query path planning. *Proceedings 2000 ICRA. Millennium Conference. IEEE International Conference on Robotics and Automation. Symposia Proceedings (Cat. No.00CH37065)*, 2: 995–1001 vol.2.
- LaValle, S.; and Kuffner, J. 2001. Randomized Kinodynamic Planning. *I. J. Robotic Res.*, 20: 378–400.
- Nagy, B.; and Kelly, A. 2001. Trajectory generation for car-like robots using cubic curvature polynomials. *Field and Service Robots*.
- Pivtoraiko, M.; and Kelly, A. 2005. Efficient constrained path planning via search in state lattices. In *International Symposium on Artificial Intelligence, Robotics, and Automation in Space*, 1–7. Munich Germany.
- Pivtoraiko, M.; Knepper, R. A.; and Kelly, A. 2009. Differentially constrained mobile robot motion planning in state lattices. *Journal of Field Robotics*, 26(3): 308–333.
- Sakcak, B.; Bascetta, L.; Ferretti, G.; and Prandini, M. 2019. Sampling-based optimal kinodynamic planning with motion primitives. *Autonomous Robots*, 43(7): 1715–1732.
- Sturtevant, N. 2012. Benchmarks for Grid-Based Pathfinding. *Transactions on Computational Intelligence and AI in Games*, 4(2): 144 – 148.
- Yakovlev, K. S.; Andreychuk, A. A.; Belinskaya, J. S.; and Makarov, D. A. 2022. Safe Interval Path Planning and Flatness-Based Control for Navigation of a Mobile Robot among Static and Dynamic Obstacles. *Automation and Remote Control*, 83(6): 903–918.

Appendix A. Proofs of Theoretical Statements

Lemma 1

Proof. To prove this lemma, it is sufficient to present the configuration of the primitives Ψ' , which we will define as follows:

1. If $k = U_{prim} - 1$, then we take the initial configuration of the primitives:

$$\Psi' = \Psi_\theta,$$

where θ is the angle at which the primitive $prim$ ends.

2. In the remaining cases, we define:

$$\Psi' = \{(prim, k+1) \mid (prim, k) \in \Psi, \\ \Delta_k^{prim} = (i' - i, j' - j)\}$$

It is now straightforward to verify from the definition of the successor relationship that $v = (i', j', \Psi')$ will be a successor of u . Moreover, v is initial only in the case when $k = U_{prim} - 1$, which is precisely what was required. \square

Lemma 2

Proof. We begin with point 1. Such a pair $(prim, k)$ must exist by the definition of the initial successor (since u_l is a successor of u_{l-1}). Therefore, it is sufficient to prove the uniqueness. Suppose there exists another pair $(prim', k) \in \Psi_{l-1}$ that satisfies all the same conditions.

First, let us consider $prim$. Since $(prim, k) \in \Psi_{l-1}$, by the definition of a successor, it follows that $(prim, k-1) \in \Psi_{l-2}$ and $\Delta_{k-1}^{prim} = (i_{l-1} - i_{l-2}, j_{l-1} - j_{l-2})$. Continuing in a similar manner, we obtain that $(prim, 1) \in \Psi_{l-k}$ and $\forall t \in \{l-k, \dots, l-1\}$ it holds that $\Delta_t^{prim} = (i_{t+1} - i_t, j_{t+1} - j_t)$.

Note that the vertex u_{l-k} exists. Indeed, since $l > 1$, among the previous vertices relative to u_l on the path, there must be at least one initial vertex (at the very least, u_1). Therefore, by continuing in a similar manner, we will inevitably reach the extended cell where $prim$ originated, namely u_{l-k} . It is also important to note that the extended cell u_{l-k} is initial, as it is either equal to u_1 (in which case the fact that u_{l-k} is initial follows from the condition) or it is a successor of some u_{l-k-1} . In this case, u_{l-k} will also be initial, as this is the only scenario according to the definition of a successor where a configuration can contain a pair of a primitive with 1. Thus, since u_{l-k} is initial, we have $\Psi_{l-k} = \Psi_\phi$ for some discrete angle ϕ .

Finally, we have obtained that $(prim, 1) \in \Psi_\phi$ and for all t such that $l-k \leq t \leq l-1$, it holds that $\Delta_t^{prim} = (i_{t+1} - i_t, j_{t+1} - j_t)$. Considering that $prim$ is a primitive of the control set (i.e., it is regarded as a motion template), the obtained result guarantees that if a copy of $prim$ is placed at (i_{l-k}, j_{l-k}) , it will yield a primitive that transitions from the discrete state $s_1 = (i_{l-k}, j_{l-k}, \phi)$ to another discrete state $s_2 = (i_l, j_l, \theta)$. Completely analogous reasoning can be applied to the primitive $prim'$. As a result, we will have two distinct primitives (since $prim$ and $prim'$ were assumed to be different) that transition from s to s' , which leads to a contradiction, as this work assumes that there can be no more than one primitive between two discrete states.

Point 2 of the theorem follows from the proven point 1. Indeed, all transitions along the path u_1, \dots, u_N lead either to a non-initial cell (in which case their cost, according to the previous section, is uniquely defined and equal to 0) or to an initial cell. However, according to point 1, there exists a unique primitive that leads to the creation of this initial cell, which means that the cost of transitioning into it is uniquely defined and equal to the cost of this primitive. \square

Theorem 3 (Main Theorem)

Proof. Let there be any trajectory composed of primitives from s to s' with a cost c (which corresponds to a path in the state lattice graph). Consider two adjacent primitives in this trajectory — the k -th and $(k+1)$ -th. They connect at some discrete state $t_k = (i_k, j_k, \phi_k)$, which is the endpoint of the k -th primitive and the beginning of the $(k+1)$ -th primitive.

Now, let us apply Theorem 1 to both primitives, yielding two paths in the mesh graph, where the initial extended cell $u_k := (i_k, j_k, \Psi_{\phi_k})$ represents the endpoint of the path corresponding to the k -th primitive and the starting point of the path corresponding to the $(k+1)$ -th primitive. Thus, these paths can also be concatenated into a single longer path. Moreover, the costs of these paths individually, according to Theorem 1, will be exactly equal to the costs of the primitives. Therefore, their combination into a single longer path will have a cost equal to the sum of the costs of these primitives.

By applying similar reasoning to all primitives in the trajectory, we conclude that there exists a path in the mesh graph between the two initial extended cells u and u' , the cost of which is equal to the total cost of the primitives in the trajectory, that is, c . Moreover, the projections of the vertices along this path precisely forming the collision trace of the trajectory (since this holds true for each primitive by Theorem 1, it is also evidently true for the entire trajectory). Therefore, the first point of the theorem is correct — such a path indeed exists and can be found.

Now, let us move on to point 2 of the theorem. Suppose the path with cost c in the mesh graph from point 1 has already been found: u_1, \dots, u_N , where $u_1 = u$ and $u_N = u'$. Theorem 2, and specifically its proof, demonstrates a method for recovering the trajectory from s to s' with a cost exactly equal to the cost of the path in the mesh graph, that is, c . The only thing that needs to be proven is that Algorithm 3 recovers the same trajectory as in the proof of Theorem 2.

Consider the proof of Theorem 2 in detail. It was conducted using the method of mathematical induction, where each step involved taking the next initial extended cell, let $u_l := (i_2, j_2, \Psi_{\theta_2})$, and then stating that there exists a unique $prim$ from the control set that satisfies certain conditions. Next, we traced back along the path in the mesh graph using this primitive, obtaining that $(prim, 1) \in \Psi_{\theta_1}$, where Ψ_{θ_1} is the configuration of primitives within another initial cell, let $p := (i_1, j_1, \Psi_{\theta_1})$ (note that there are no other initial extended cells between p and u_l ; otherwise, $prim$ would not be able to transition from p to u_l).

After that, it was stated that if a copy of $prim$ is placed at the point (i_1, j_1) , it will yield a primitive whose collision

trace precisely coincides with the projections of the vertices along the path from p to u_l . This means that such a primitive starts at the point (i_1, j_1) and ends at (i_2, j_2) , thus transitioning between the discrete states $s_1 := (i_1, j_1, \theta_1)$ and $s_2 := (i_2, j_2, \theta_2)$ (since, due to the initial configurations Ψ_{θ_1} and Ψ_{θ_2} , this primitive starts and ends at angles θ_1 and θ_2 , respectively). As a result, this primitive extends the segment of the trajectory from the previous step of the mathematical induction.

Finally, it is important to note that Algorithm 3 does the same thing — it sequentially considers all pairs of neighboring initial cells denoted as p and u_l along the path in the mesh graph, and then reconstructs the primitive between the discrete states s_1 and s_2 , the existence of which was just derived from the proof of Theorem 2 (and the uniqueness of this primitive follows from the assumption in this work that there can be no more than one primitive between two discrete states). Thus, Algorithm 3 will reconstruct exactly the same trajectory as in the proof of Theorem 2, meaning that this trajectory satisfies all the conditions of that theorem, which concludes this proof. \square

Appendix B. Practical Implementation

According to Theorem 3, our proposed MeshA* algorithm consists of pathfinding on the mesh graph using the standard and widely used A* algorithm, followed by the reconstruction of the chain of primitives using Algorithm 3. In this section, we will present the implementation details of MeshA*, which ensure its high efficiency.

Numbering Configurations of Primitives

It is important to note that the configuration of the primitives Ψ is a complex object to utilize directly in the search process. However, it is evident that there is a finite number of such configurations (since the number of primitives in the control set is finite), allowing us to assign a unique number to each configuration and use only this number in the search instead of the complex set.

According to Theorem 3, we are only interested in paths originating from some initial extended cell. Therefore, it makes sense to number only the configurations that are reachable from these extended cells (which will be defined more formally below). To achieve this, we can fix a set of extended cells with all possible initial configurations of the primitives (the number of which corresponds to the number of discrete headings) and then perform a depth-first search from each of these cells. This search will assign a number to each newly encountered configuration while stopping at already numbered configurations. The pseudocode for the described idea is implemented in Algorithm 4.

Theorem 4. *For any extended cell $u' = (i', j', \Psi')$ that is reachable from some initial extended cell $u = (i, j, \Psi_\theta)$ via a path on the mesh graph, Algorithm 4 will assign a number to the configuration of primitives Ψ' :*

$$\Psi' \in \text{MainProcedure}()$$

Note: All such Ψ' (which are in the extended cell reachable from some initial one) are referred to as reachable.

Algorithm 4: Numbering Configurations of Primitives

Output: Dictionary *Numbers* that maps each configuration of primitives to its corresponding number.

Function name: MainProcedure()

```

1:  $n = 0$  ▷ Initialize the variable for the number
2:  $Numbers \leftarrow \{\}$ 
3: for all discrete heading  $\theta$  do
4:    $\Psi \leftarrow \text{InitConf}(\theta)$ 
5:    $u \leftarrow (0, 0, \Psi)$  ▷ Next initial cell
6:    $\text{NumberingDFS}(u)$  ▷ Start the DFS defined below
7: end for
8: return  $Numbers$ 

```

Function name: NumberingDFS(u)

```

1:  $i, j, \Psi \leftarrow u$ 
2: if  $\Psi \in Numbers$  then
3:   return
4: end if
5:  $Numbers[\Psi] = n$ 
6:  $n \leftarrow n + 1$ 
7: for all  $v, cost \in \text{GetSuccessors}(u)$  do
8:    $\text{NumberingDFS}(v)$ 
9: end for

```

Proof. Let the path on the mesh graph, as mentioned in the condition, be of the form u_1, \dots, u_N , where $u_l := (i_l, j_l, \Psi_l)$ for any $l \in [1, N]$. In this case, $i_1 = i, j_1 = j, i_N = i', j_N = j'$, and $\Psi_1 = \Psi_\theta, \Psi_N = \Psi'$. Note that the mesh graph is regular (i.e., invariant under parallel translation), so we can assume $i = 0, j = 0$ (we can always consider such a parallel translation to move (i, j) to $(0, 0)$); the successor relationship in the mesh graph does not depend on the parallel translation, which is the essence of regularity, and thus the sequence u_1, \dots, u_N will remain a path after such a shift).

Now, we will proceed by contradiction. Suppose $\Psi_N = \Psi'$ is not numbered. Consider the chain of configurations of primitives Ψ_1, \dots, Ψ_N . Let Ψ_l be the first configuration in this chain that has not been assigned a number. Note that $u_1 = (0, 0, \Psi_\theta)$ is one of the extended cells that the MainProcedure will take at line 5, and from which it will launch NumberingDFS at line 6. The latter will assign a number to the configuration Ψ_θ at line 5, so $\Psi_1 = \Psi_\theta$ is certainly numbered, which means $l > 1$.

In this case, we conclude that Ψ_{l-1} exists and is also numbered, meaning that for some extended cell $v := (i'', j'', \Psi_{l-1})$, NumberingDFS(v) was launched. However, in line 7 of this procedure, all successors of v must have been considered. Since $u_l = (i_l, j_l, \Psi_l)$ is a successor of $u_{l-1} = (i_{l-1}, j_{l-1}, \Psi_{l-1})$, and the successor relationship do not depend on specific coordinates due to regularity, there must be an extended cell among the successors of v with the configuration Ψ_l . Therefore, NumberingDFS should have been launched from it in line 8, which would assign it a number. This leads us to a contradiction, thus proving the theorem. \square

Thus, the MainProcedure will number all configura-

tions of primitives that may occur during the pathfinding process for trajectory construction (since, as stated in Theorem 3, we only search for paths from the initial extended cell). Therefore, MeshA* can work with these numbers instead of the configurations of primitives to simplify operations, thereby accelerating the search.

Precomputing Stage

For the efficient operation of the MeshA* algorithm, a pre-computation stage is required, which is performed once for a fixed control set and then reused across various maps for any tests. Thus, this stage is not different from the process of generating the control set itself.

The primary objective of this stage is to obtain the numbers for all configurations according to Algorithm 4. We also recommend storing the following information during this numbering process:

1. For each discrete heading θ , store the number of the initial configuration Ψ_θ .
2. It is important to note that the mesh graph is regular, meaning it is invariant under parallel translation. This implies that for any extended cell $u := (i, j, \Psi)$ and its successor $v := (i', j', \Psi')$, the values $\delta_i = i' - i$ and $\delta_j = j' - j$ do not depend on the original coordinates (i, j) . Therefore, for each Ψ , it is sufficient to store $(\delta_i, \delta_j, \Psi')$ corresponding to each of its successors. This allows us to instantly derive the successors of any extended cell (a, b, Ψ) as $(a + \delta_i, b + \delta_j, \Psi')$. Consequently, we propose that during the configuration numbering process in Algorithm 4, for number of each configuration Ψ , to store the numbers of the successor configurations, along with the shifts δ_i and δ_j .

Additionally, if Mesh/ParallA* or Mesh/PruningA* is planned for use, the same stage can be utilized to define the rule for identifying soft duplicates. For instance, according to our previously mentioned method, we should obtain the set of vertices reachable from $(0, 0, \Psi)$ in ≤ 2 steps, and then derive the corresponding set of grid cells from their projections. At this stage we can number all these sets (since the number of distinct Ψ is finite), resulting in a unique identifier. Thus, to determine whether two extended cells $(0, 0, \Psi)$ and $(0, 0, \Psi')$ are soft duplicates, it is sufficient to compare the identifiers corresponding to Ψ and Ψ' . Again, due to the regularity of the mesh graph, these same identifiers can be used to ascertain whether the extended cells (i, j, Ψ) and (i, j, Ψ') with shared coordinates (for any i, j) are soft duplicates.

A* implementation

Any A* algorithm involves sequentially expanding (i.e., considering successors of) each vertex in the graph in a certain order until the goal vertex, for which we are searching for a path, is encountered. Additionally, during the execution of the A* algorithm, a heuristic function h must be computed for each vertex, which estimates the cost of the remaining path from that vertex to the goal vertex. In this section, we will present several optimizations of A* as applied to the case of searching on the mesh graph.

Consider an initial cell $u := (i, j, \Psi_\phi)$ and suppose we want to find a path to the goal vertex $v := (i', j', \Psi_\theta)$ (which is an initial cell, as according to Theorem 3, we are only interested in paths that end at initial extended cells). We note that the heuristic value $h(u)$, which estimates the cost of the path from u to v , can be taken as the same value that estimates the cost of the path on the state lattice from $s := (i, j, \phi)$ to $s' := (i', j', \theta)$, as the previous sections have effectively demonstrated the existence of a bijection (preserving cost) between such paths.

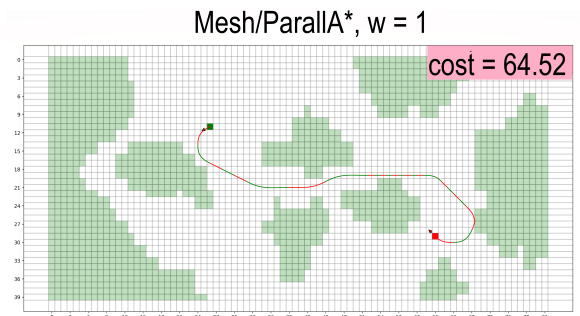
Now, let us consider an arbitrary non-initial extended cell $u := (i, j, \Psi)$ (to which A* has already found a path from some initial extended cell from which the search began). Let $\Psi = \{(prim_1, k), \dots, (prim_r, k)\}$. It is important to note that from u , exactly r distinct initial extended cells (corresponding to the end of each $prim_l$, where $l = 1, \dots, r$) can be reached directly (i.e., without intermediate initial extended cells), which we will denote as u_1, \dots, u_r . Since we are only interested in paths to some initial extended cell, the first initial cell from u on any such path will be some u_l (where $l = 1, \dots, r$). Moreover, the segment of the path from u to this u_l will have a cost equal to c_{prim_l} due to the definition of costs on the mesh graph. Therefore, the estimate $h(u)$ for the cost of the path from u to the goal vertex can be defined as $h(u) := \min_{l=1, \dots, r} (h(u_l) + c_{prim_l})$. It is worth noting that this definition does not compromise either the consistency or the admissibility of the original heuristic h (which was defined only on the state lattice), thus preserving the optimality guarantees of the A* algorithm. Thus, we have shown that any heuristic h that was defined solely on the state lattice graph can be extended to the mesh graph while preserving all guarantees. This further ensuring straightforward application of our approach.

Additionally, if all u_l (for $l = 1, \dots, r$) have already been expanded by the A* algorithm, there is no point in expanding u . This important optimization significantly accelerates the search.

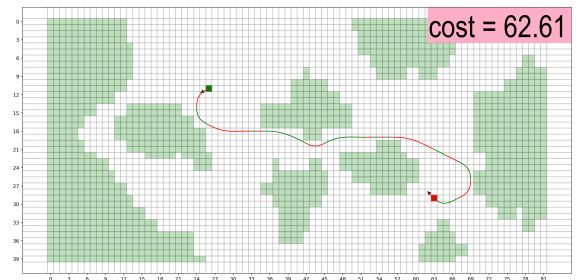
The final optimization of A* worth mentioning is as follows. Note that Algorithm 3, which reconstructs the trajectory, only uses initial extended cells in the path. This means that there is no need to store the other cells in memory.

Appendix C. Pathfinding Examples

Here, we will demonstrate several examples of trajectories found by each of the algorithms for $w = 1$ and $w = 2$. In all examples, the map, as well as the initial and final states, remain the same.



LBA*, $w = 1$



MeshA*, $w = 1$

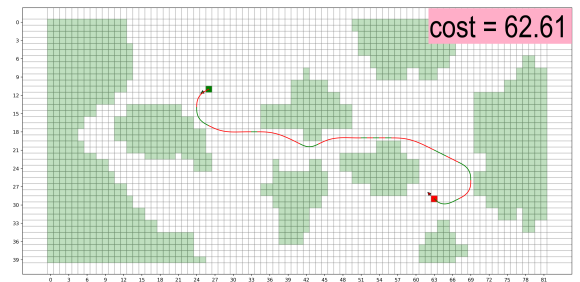
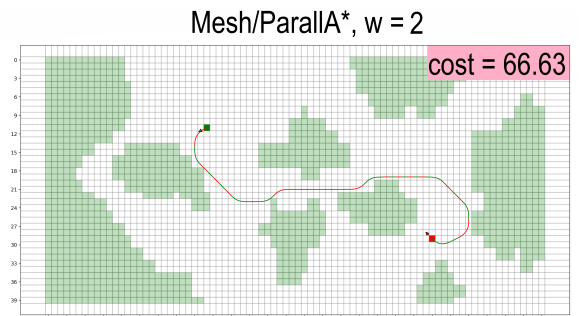
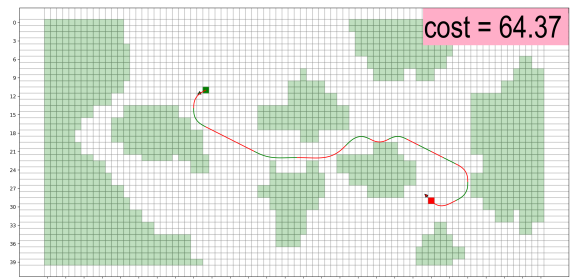


Figure 6: Examples for $w = 1$



LBA*, $w = 2$



MeshA*, $w = 2$

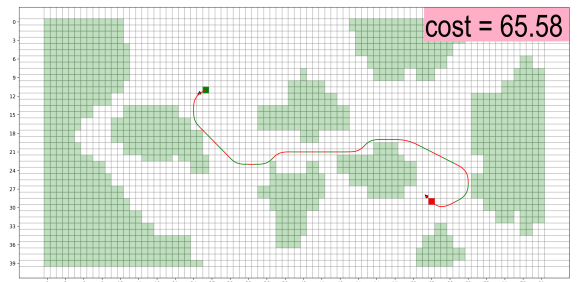


Figure 7: Examples for $w = 2$